E-Cadherin Accumulation within the Lymphovascular Embolus of Inflammatory Breast Cancer Is Due to Altered Trafficking

YIN YE[1], JOSEPH D. TELLEZ[1], MARIA DURAZO[1], MEAGAN BELCHER[1], KURTIS YEARSLEY[2] and SANFORD H. BARSKY[1,3,4]

[1]*Department of Pathology, University of Nevada School of Medicine, Reno, NV 89557, U.S.A.;*
[2]*Department of Pathology, Ohio State University, Columbus, OH 43210, U.S.A.;*
[3]*Department of Pathology, The Whittemore-Peterson Institute, Reno, NV 89557, U.S.A.;*
[4]*Department of Pathology, Nevada Cancer Institute, Las Vegas, NV 89135, U.S.A.*

Abstract. *E-Cadherin functions as a tumor suppressor in some invasive breast carcinomas and metastasis is promoted when its expression is lost. It has been observed, however, that in one of the most aggressive human breast cancers, inflammatory breast cancer (IBC), E-cadherin is overexpressed and this accounts for the formation of the lymphovascular embolus, a structure efficient at metastasis and resistant to chemotherapy through unknown cytoprotective mechanisms. Studies using a human xenograft model of IBC, MARY-X, indicate that the mechanism of E-cadherin overexpression is not transcriptional but related to altered protein trafficking. By real-time RT-PCR, E-cadherin transcript levels in MARY-X were 3- to 11-fold less than in other E-cadherin positive human breast carcinoma lines but the protein levels were 5- to 10-fold greater. In addition, several smaller E-cadherin protein fragments, e.g. 95 kDa, were present. To explain these observations, it was hypothesized that there may be altered protein trafficking. A real-time RT-PCR screen of candidate molecules generally known to regulate protein trafficking was conducted. The screen revealed 3.5- to 7-fold increased ExoC5 level and 10 to 20 fold decreased HRS and RAB7 levels, which was confirmed in human microdissected lymphovascular emboli. Since these alterations may only be correlative with E-cadherin overexpression, one of the molecules, Rab7, was selectively knocked down in MCF-7 cells. An increase in the full length 120 kDa E-cadherin and the de novo appearance of the 95 KD band were observed. These findings suggest that it is the altered E-cadherin trafficking that contributes to its oncogenic rather than suppressive role in IBC.*

Correspondence to: Sanford H. Barsky, MD, Department of Pathology, University of Nevada School of Medicine, Whittemore-Peterson Institute and Nevada Cancer Institute, 1 Manville Medical Building, University of Nevada, Reno/0350, Reno, NV 89557-0350, U.S.A. Tel: +1 7757844068, Fax: +1 7757841636, e-mail: sbarsky@medicine.nevada.edu

Key Words: HRS, RAB7, EXOC5, RT-PCR, E-cadherin, fragments.

E-Cadherin, an adhesion protein present in normal epithelial cells within lateral junctions *(zona adherens)*, is thought to function as a tumor suppressor in certain types of invasive breast carcinomas and metastasis is promoted when its expression is lost by gene mutation, promoter methylation or promoter repression by snail/slug and other mediators of epithelial-mesenchymal transition (EMT) (1-3). However, in the vast majority of human breast cancers, E-cadherin expression is not lost, but retained. In fact, the presence of E-cadherin immunoreactivity is routinely used to diagnose ductal carcinoma *in situ* (DCIS) and infiltrating ductal carcinoma where it is present, in contrast to lobular carcinoma *in situ* (LCIS) and infiltrating lobular carcinoma, where it is lost.

It has also been observed that in one of the most aggressive and metastatic human breast cancers, inflammatory breast cancer (IBC), E-cadherin is not only retained but overexpressed and distributed circumferentially 360˚ around the cancer cell membrane (4-6). This distribution accounts for the formation of the lymphovascular embolus. Lymphovascular emboli of both IBC as well as non-IBC tumors strongly express E-cadherin. The lymphovascular embolus is a structure efficient at metastatic dissemination and resistant to chemotherapy/radiotherapy through ill-defined cytoprotective mechanisms. E-cadherin seems to be a very important molecule for tumor cell survival. The mechanism of the overexpression of E-cadherin in IBC had not been previously investigated. This study used the human xenograft model of IBC, MARY-X (4-9), and other common, well established E-cadherin-positive and -negative human breast carcinoma cell lines to investigate the mechanism of E-cadherin overexpression in IBC and in the lymphovascular embolus.

Materials and Methods

Cell lines and xenograft studies. MARY-X was previously established from a patient with IBC and exhibited the phenotype of florid lymphovascular invasion with tumor emboli formation in nude/SCID mice (4-6). MARY-X gave rise to tight aggregates of tumor cells termed spheroids *in vitro*, which were propagated in suspension culture. These spheroids were maintained for periods up to 3 months by growing them in either keratinocyte serum-free medium with supplements (Life Technologies, Inc., Gaithersburg, MD, USA), or in minimal essential medium with 10% fetal calf serum (Life Technologies, Inc.). The spheroids exhibited high cell density (10^3 cells in a 120 μm diameter spheroid); remained viable in suspension culture for 12 weeks; never formed monolayers on either plastic, extracellular matrix-coated dishes or feeder layers of fibroblast, myoepithelial, or endothelial cells; and fully recapitulated the MARY-X phenotype of lymphovascular emboli when re-injected into nude/SCID mice. The crude minced fragments of MARY-X contained spheroids ranging in size from 10 μm to 600 μm. Spheroids of homogeneous size were obtained by filtration through variously sized filters (Becton Dickinson, Franklin Lakes, NJ, USA). A 100 μm filter was used to exclude spheroids greater than 100 μm; the filtrate was then subsequently passed through 40 μm and 20 μm filters, which isolated 20-40 μm spheroids and >40 μm spheroids. Within these spheroids, the individual tumor cells were held together by an overexpressed E-cadherin axis (4-9) which if neutralized with anti-E-cadherin or ethylenediaminetetraacetic acid, released individual single cells. It was assumed in the past that the basis of E-cadherin overexpression in MARY-X and the MARY-X spheroids was transcriptional in nature. However, because of the unique contribution of E-cadherin to the MARY-X phenotype of florid lymphovascular emboli *in vivo* and spheroids *in vitro*, this assumption was not made in the present study. The E-cadherin expression in MARY-X and MARY-X spheroids was compared with its expression in other E-cadherin-positive (MCF-7, HTB20, HTB27 and HCC202) and E-cadherin-negative (MDA-MB-231 and MDA-MB-468) breast carcinoma cell lines. All these latter cell lines were obtained from the American Type Culture Collection (Manassas, VA, USA). All cell lines were grown in Dulbecco's modified Eagle's medium containing 10% fetal calf serum and antibiotics (100 units/ml penicillin and 100 mg/ml streptomycin) at 37˚C in a 5% CO_2 atmosphere at constant humidity.

RNA isolation and cDNA synthesis. Total RNA was isolated from cultured cells using an RNeasy Mini Kit (Qiagen, Valencia, CA, USA) according to the manufacturer's instructions. Total RNA was eluted and dissolved in RNase-free water, and the concentration was determined using a NanoDrop® spectrophotometer (NanoDrop Technologies, Wilmington, DE, USA). For the first-strand cDNA synthesis, the SuperScript® III First-Strand Synthesis System (Invitrogen, Inc., Carlsbad, CA, USA), oligo$(dT)_{20}$ and 2 μg of total RNA were used. The synthesized cDNA was used for real-time RT-PCR analysis of relative expression levels of target genes.

Real-time RT-PCR. Real-time RT-PCR was performed on an ABI 7500® real-time PCR system (Applied Biosystems, Foster City, CA, USA). Briefly, cDNA was combined with primer sets and the ABI Power SYBR Green PCR Master Mix. The following conditions were used: an initial denaturation at 95˚C for 5 min followed by denaturation at 94˚C for 30 s, annealing at 58˚C for 30 s, and extension at 68˚C for 1 min for a total of 40 cycles. PCR products were analyzed on a 2.0% agarose gel. Gene expression levels were calculated relative to the housekeeping gene β-actin by using ABI 7500® System SDS software. All real time RT-PCR experiments were performed with a minimum of five replicates and results depicted as mean±standard deviation. The primers used were as follows:

RAB11	Sense	GGA AAG CAA GAG CAC CAT TGG AGT
	Antisense	TTT GTA GAG TCT AGG GCC GAA GTT TC
SRC	Sense	TCA ACA ACA CAG AGG GAG ACT GGT
	Antisense	TTT CGT GGT CTC ACT TTC TCG CAC
NM23	Sense	GCC AAC TGT GAG CGT ACC TTC ATT
	Antisense	TAT GCA GAA GTC TCC ACG GAT GGT
RALA	Sense	TTC CAG GCG ACA AGG ACC GAG TA
	Antisense	CCA TCT AGC ACT ACC TTC TTC CGA
RAB5	Sense	ACC ACC GCC ATA GAT ACA CTC TCA
	Antisense	ACT AGG CTT GAT TTG CCA ACA GCG
RAB7	Sense	AGT TCC CTG GAA CCA GAA CTT GGA
	Antisense	TGT GAC TAG CCT GTC ATC CAC CAT
HRS	Sense	AAG AAC CCA CAC GTC GCC TTG TAT
	Antisense	CAG CAA ACA TGG CAT CGC TCT CTT
EXOC2	Sense	ACC GAC CTC ATA GGC TTG ACC ATT
	Antisense	ACA AGG GCG GAA TTC CTT TGT TCC
EXOC4	Sense	AAA GGG TCG CCT TGA AGA AGC CTA
	Antisense	CAG TTT CCG AAG CTC ATC CCG TTT
EXOC5	Sense	TGA ACG TCT TGT ATG GAG AAC CC
	Antisense	TAA CTG GTC TCC AAG GTG ACA GAC
EXOC6	Sense	CCA ACC GAA GGT TTC AAG ATG CTG
	Antisense	AAC CGG TAT TGA CTA ACC CAG GGA
EXOC7	Sense	AGA TTG AGG ACA AGC TGA AGC AGG
	Antisense	TGG CCA CAT GGT AGT AGC TGA TGA
ARF6	Sense	TCT CAC CGC GAG GGA GAC TG
	Antisense	GCA GAA CTG GGA GGA GGA GTT
CDH1	Sense	GTC ACT GAC ACC AAC GAT AAT CCT
	Antisense	TTT CAG TGT GGT GAT TAC GAC GTT A
ACTB	Sense	GGC ACC CAG CAC AAT GAA G
	Antisense	GCC GAT CCA CAC GGA GTA CT

Immunocytochemical studies and Western blot analysis. For the immunocytochemical studies on the MARY-X spheroids, primary murine monoclonal antibodies included anti-human E-cadherin (clone HECD-1, unconjugated; Zymed Laboratories, Inc., South San Francisco, CA, USA). Control antibodies included mouse IgG_1 (clone ×40, unconjugated; BD Pharmingen, San Diego, CA, USA). Secondary antibodies included fluorescein isothiocyanate-conjugated goat antimouse IgG (BD Pharmingen). For the immunofluorescence

studies, MARY-X spheroids were fixed in cold methanol:acetone (1:1) for 20 min. Cells were blocked with phosphate-buffered saline (PBS) plus 1% normal donkey serum for 30 min and followed by incubation with the respective antibodies for 45 min. For the unconjugated antibodies, incubation with secondary antibody occurred for 30 min. The nuclei were counterstained with Hoechst 33342 dye (5 g/ml) (Sigma-Aldrich, St. Louis, MO, USA). The stained cells were imaged on a Nikon E600 DIC Dual View microscope with an attached Roper CoolSnap CCD camera (Nikon Instruments, Melville, NY, USA) and MetaVue software (Universal Imaging Corporation, Downington, PA, USA). For the Western blot studies, antibodies against E-cadherin (H-108) and RAB7 (H-50), were obtained from Santa Cruz Biotechnology (Santa Cruz, CA, USA). Secondary antibodies and Western blotting substrates were obtained from Pierce Technology Inc. (Rockford, IL, USA). To prepare protein lysates from cell lines, cells were lysed using ice-cold RIPA lysis buffer (Pierce Biotechnology, Inc.). Protein content was determined using BCA protein assay (Pierce Biotechnology, Inc.), and samples were stored at –80˚C. For Western blot analysis, boiled protein was loaded onto a 4-12% Precast gradient gel, transferred to nitrocellulose membranes (Invitrogen Corporation, Inc.) and incubated with antibodies. Bound antibodies were detected by a chemiluminescent detection system (West Femto; Pierce Biotechnology, Inc.) according to the manufacturer's instructions.

RNA interference. Knockdown of RAB7 was achieved with an RNAi (RNA interference) approach, using small interfering RNA (siRNA) for transient, but effective knockdown. For the siRNA-knockdown experiments, RAB7 siRNA sequences included: 5'-GCUGCGUUC UGGUAUUUGAtt-3' (sense) and 5'-UCAAAUACCAGAACGC AGCag-3' (antisense). MCF-7 cells were transfected with 50 nM of either control siRNA (NCSI) or RAB7 siRNA. After 48 h, the cells were collected and analyzed for the expression of RAB7 by both real-time RT-PCR and Western blot.

Analysis of human material. Ten cases of primary human inflammatory breast cancer and five cases of non-IBC but with florid lymphovascular emboli were selected from the Information Warehouse patient database at Ohio State University Medical Center maintained in CoPath, Sunquest Information Systems, Inc., Tucson, USA and anonymized. All references to real patient identity were removed before study. These tissues were available as archival paraffin blocks and sectioned. Standard immunohistochemical protocols for E-cadherin were used. The antibody used was an anti-human E-cadherin (clone HECD-1, unconjugated; Zymed Laboratories, Inc., South San Francisco, CA, USA). The appropriate secondary antibody was used and the detection system applied was a peroxidase-conjugated streptavidin-biotin complex. Visualization occurred after the application of a DAB brown chromogen. Subsequent laser capture microdissection of the lymphovascular embolic areas and non-embolic areas were carried out using a Veritas™ microdissection instrument (Molecular Devices, Sunnyvale, CA, USA). 250 emboli from 10 cases of IBC and 5 cases of non-IBC consisting of a mean of 100 cells/embolus and control non-embolic areas were captured, pooled and subjected to RNA isolation, cDNA synthesis and real time RT-PCR analysis.

Institutional approvals. All animal and *in vitro* studies were approved by The Ohio State University's Animal Care and Use Committee, protocol 2007A0218 and by The Ohio State University's Institutional Biosafety Committee, protocol 2007R0057. Additional animal studies were approved by the University of Nevada, Reno's Institutional Animal Care and Use Committee, protocols 00439 and 00440.

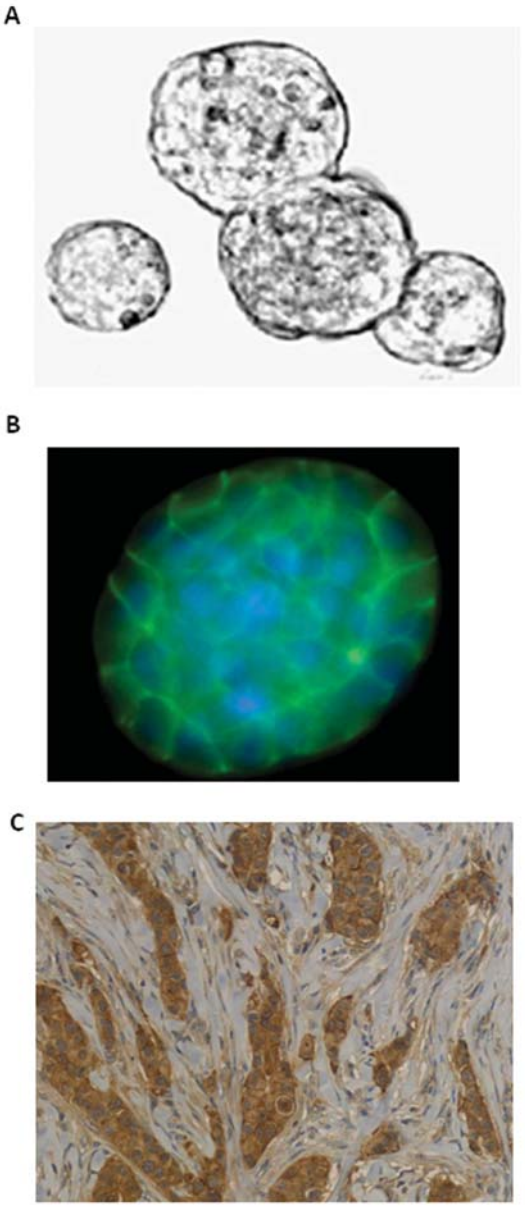

Figure 1. *A: Phase-contrast of MARY-X spheroids in suspension culture reveals tight aggregates of individual tumor cells held together by overexpressed E-cadherin. B: Immunofluorescence with anti-E-cadherin reveals prominent membrane immunolocalization of E-cadherin (green fluorescence) within the spheroids distributed 360˚ around the cells. Hoechst 33342 nuclear counterstain demonstrated central nuclear staining in this composite image. C: Immunoperoxidase with anti-E-cadherin in a typical case of human IBC demonstrates strong membrane E-cadherin immunoreactivity in tumor cell clumps, some of which represent lymphovascular tumoral emboli.*

Statistical analysis. Declarations of differences imply differences of statistical significance. For the comparative studies of mRNA and protein levels of E-cadherin and its trafficking-regulatory molecules among the different human breast carcinoma cell lines, significance was assessed by Student's *t*-test and ANOVA. *p*-Values <0.05 were judged to the statistically significant. SAS Analytics Software was used in the analysis (SAS Institute, Inc., CARY, USA).

Results

E-Cadherin overexpression produces the IBC phenotype. E-cadherin over-expression was responsible for the tight aggregates of the MARY-X spheroids *in vitro* (Figures 1A and 1B) as well as for the lymphovascular emboli *in vivo* (Figure 1C).

The mechanism of E-cadherin overexpression is not transcriptional. By real-time RT-PCR, E-cadherin mRNA levels were unexpectedly less in MARY-X and the MARY-X spheroids than in a number of different E-cadherin-positive human breast carcinoma cell lines including HTB20, HTB27, HCC202 and MCF-7, but expectedly more than in the E-cadherin-negative lines (MDA-MB-231 and MDA-MB-468) (Figure 2A). By Western blot analysis, however, the MARY-X and MARY-X spheroids exhibited 5- to 10-fold greater protein levels than any of the other E-cadherin-positive cell lines (Figure 2B). Increased levels of E-cadherin fragments were also observed (Figure 2B). Because MARY-X spontaneously forms spheroids *in vitro* whereas the other cell lines normally grow as monolayers, spheroid formation was induced in the other lines with previously established methods (9) in order to compare their spheroid state with the spheroid state of MARY-X. The protein levels of E-cadherin were not altered by the induction of spheroidgenesis in these other cell lines (data not shown) and the protein levels of the MARY-X spheroids remained unsurpassed.

The mechanism of E-cadherin overexpression involves its re-distribution. Not only were the levels of E-cadherin protein substantially increased in MARY-X and its derived spheroids but also the distribution of E-cadherin was strikingly altered compared to normal epithelial cells within ducts and acini. In normal epithelial cells, E-cadherin localized to the lateral junctions which were present focally along the lateral border between epithelial cells (data not shown). But in MARY-X and its derived spheroids, E-cadherin escaped the confines of the lateral junctions and was present circumferentially 360˚ around the plasma membrane of the cancer cell (Figure 1B). E-Cadherin similarly escaped the confines of the lateral junctions and was present circumferentially 360˚ around the plasma membranes of the cells contained within the lymphovascular emboli of IBC (Figure 1C).

The mechanism of E-cadherin overexpression and re-distribution involves altered trafficking. To explain these observations, it was hypothesized that E-cadherin trafficking may be altered in MARY-X and its derived spheroids. A real-time RT-PCR screen of molecules thought to regulate protein trafficking was conducted (Figure 3). The results of this screen demonstrated that EXOC5 was significantly increased 3.5- to 7-fold (p=0.01) (Figure 3D), and both (HGS) and Rab7 were significantly decreased 10 to 20 fold (p=0.01) (Figures 3G and

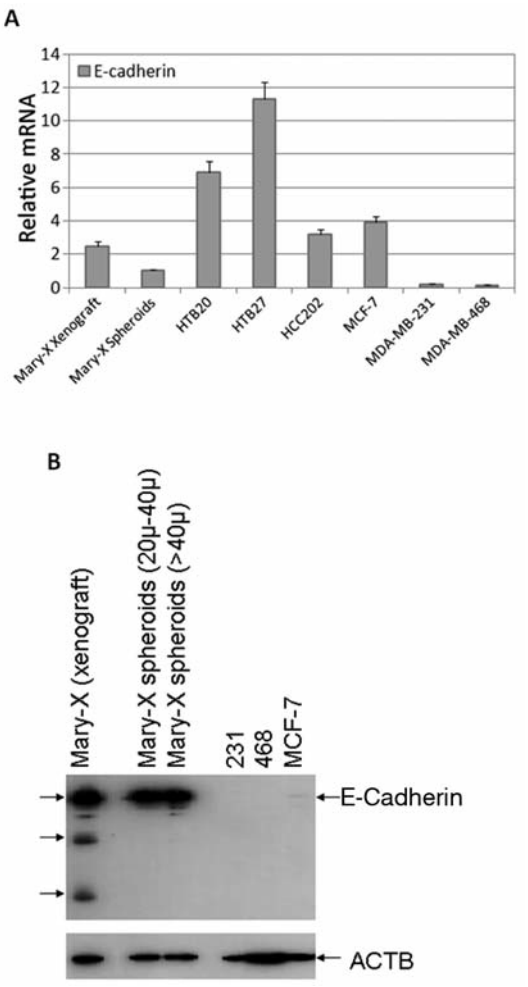

Figure 2. *A: Real time RT-PCR indicates relative transcript levels of E-cadherin in MARY-X and MARY-X spheroids to be significantly and unexpectedly less than in other E-cadherin-positive cell lines but expectedly more than in E-cadherin negative cell lines whose expressions were near zero. Results depict mean±standard deviation of five experiments. B: In contrast, protein levels by Western blot in both MARY-X and different sized MARY-X spheroids (20-40 μm, >40 μm) were increased 5- to 10-fold compared to E-cadherin-positive and E-cadherin-negative cell lines. Other E-cadherin-positive cell lines were similar to MCF-7 in terms of their levels of E-cadherin protein. Western blot was purposely underexposed due to the intense signals of the MARY-X xenograft and spheroids so that the MCF-7 signal was comparatively weak. Note also the E-cadherin fragments (arrows) in MARY-X and its spheroids. β-actin (ACTB) was used as a housekeeping control.*

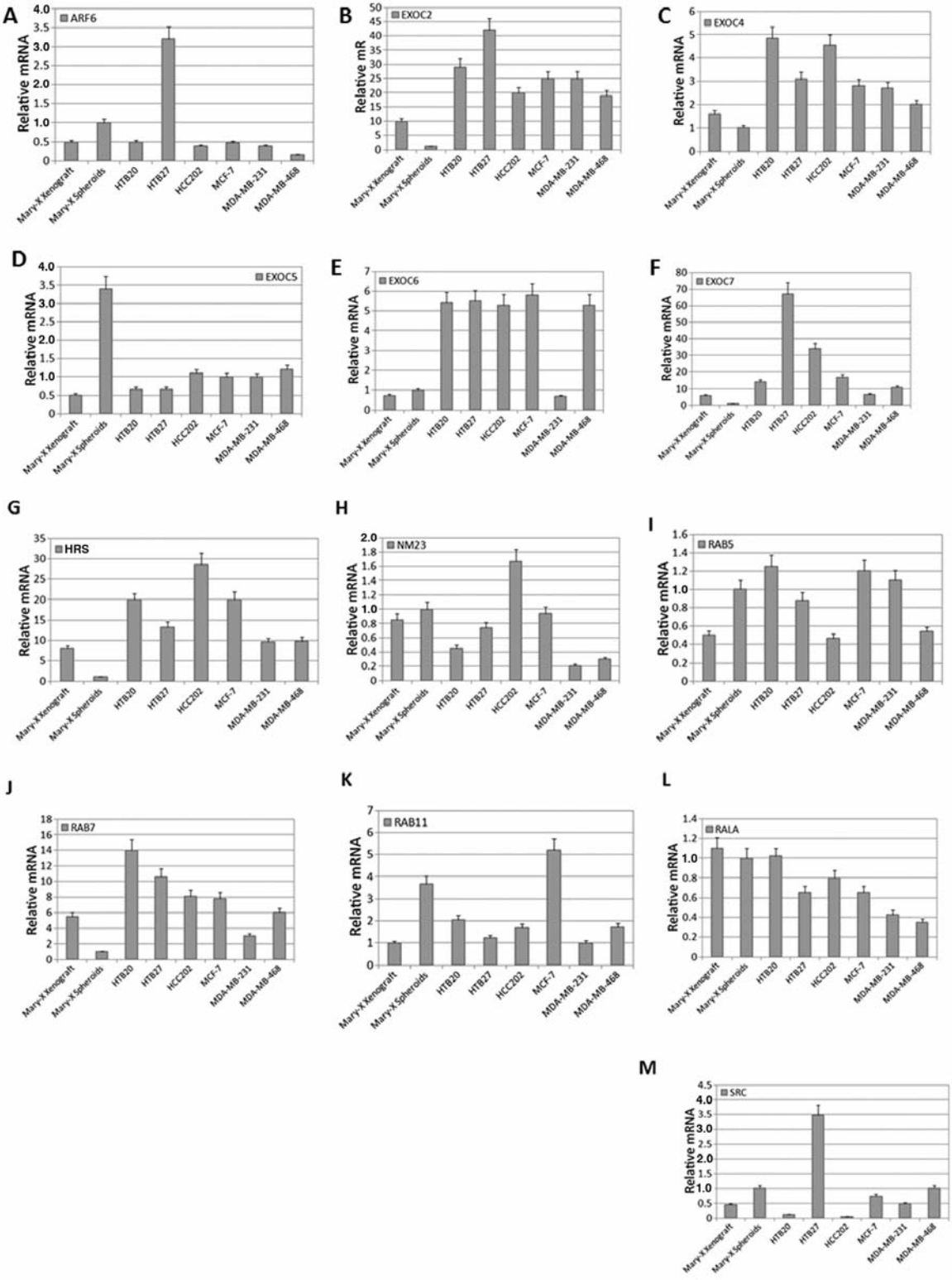

Figure 3. *Real time RT-PCR indicates relative transcript levels of indicated molecules thought to be involved in different aspects of molecular trafficking. A: ARF6; B: EXOC2; C: EXOC4; D: EXOC5; E: EXOC6; F: EXOC7; G: HRS; H: NM23; I: RAB5; J: RAB7; K: RAB11; L: RALA; M: SRC. Of this molecular screen, the relative transcript levels of three molecules were significantly different in the MARY-X spheroids compared to the other cell lines: Levels of EXOC5 were increased and levels of HRS and RAB7 were decreased (p=0.01). Results depict mean+ standard deviation of five experiments.*

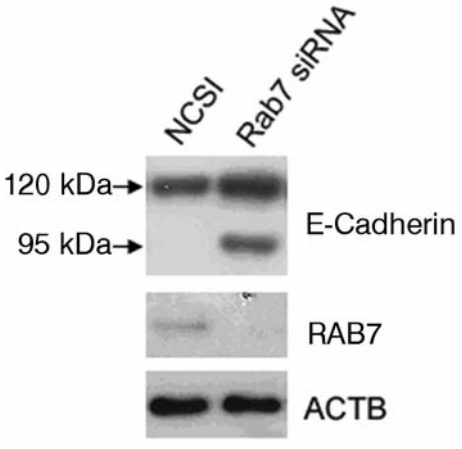

Figure 4. *Knockdown of RAB7 in MCF-7 cells. Transient RAB7 knockdown with siRNA resulted in near total knockdown of RAB7 by Western blot compared with negative control (NCSI) knockdown (middle panel). The results of RAB7 knockdown produced an increase in full length (120 kDa) E-cadherin as well as the de novo appearance of a 95 kDa fragment compared with NCSI knockdown (upper panel). β-Actin (ACTB) was used as a housekeeping control for protein loading (lower panel).*

3J) in MARY-X spheroids. These proteins are thought to play key roles in regulating lysosomal degradation and endosomal recycling. The other molecules tested, which included ARF6, NM23, RAB5, RAB11, RALA and SRC, showed no significant decreases compared to RAB7 and HRS in the MARY-X spheroids (Figures 3A, 3H, 3I, 3K, 3L and 3M). The other molecules tested, which included EXOC2, EXOC4, EXOC6 and EXOC7, showed no significant increases compared to EXOC5 in the MARY-X spheroids (Figures 3B, 3C, 3E and 3F). Since these molecular alterations which were present in the MARY-X spheroids may only be correlative with E-cadherin overexpression and redistribution, the expression of one of these molecules, RAB7, was modulated by knocking it down in MCF-7 cells to see the effects on E-cadherin expression. This knockdown was achieved effectively (Figure 4) and resulted not only in an increase in full length E-cadherin but also the *de novo* appearance of its 95 kDa fragment (Figure 4), a fragment which was also observed in MARY-X (Figure 2B).

The mechanism of E-cadherin overexpression, redistribution and altered trafficking is applicable to lymphovascular emboli in IBC and non-IBC cases. Real-time RT-PCR studies of pooled microdissected lymphovascular emboli from both IBC as well as non-IBC cases revealed a 3-fold increase in EXOC5 (p=0.01) and a 5- to 10-fold decrease in RAB7 and HRS, respectively, compared to non-embolic areas of the non-IBC cancers (p=0.01) data not shown. With respect to these trafficking molecules, the findings in the actual lymphovascular emboli from the human cases resembled the findings in the MARY-X spheroids.

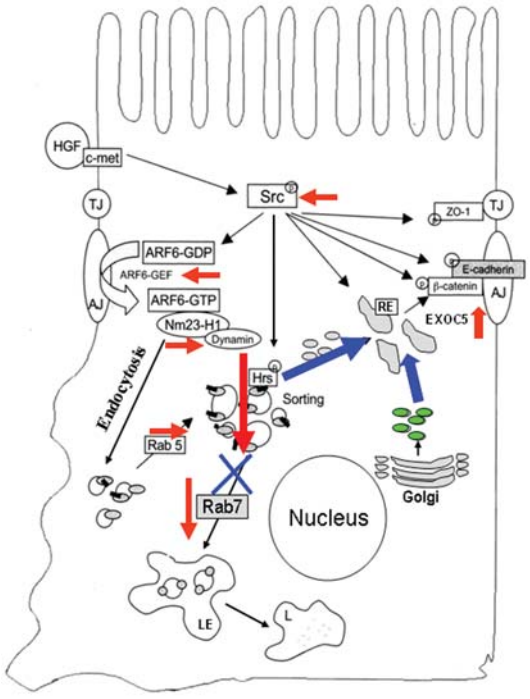

Figure 5. *Schematic depicts altered E-cadherin molecular trafficking due to decreased HRS and RAB7 (marked by down-pointing red arrows) and increased EXOC5 (marked by up-pointing red arrow). Decreased HRS and RAB7 results in significantly decreased lysosomal degradation (marked by blue cross). This decreased lysosomal degradation results in shuttled E-cadherin to the recycling endosomes (marked by blue arrow). Increased EXOC5 also results in increased endosomal recycling of E-cadherin (also marked by blue arrows). The net effect is 360° membrane accumulation of E-cadherin due to altered trafficking. [Reproduced and amended with permission from the American Society for Microbiology; model was adapted from (21)]*

Discussion

The hypothesis suggested by the present study is that E-cadherin is overexpressed in MARY-X and its derived spheroids because key proteins which regulate E-cadherin trafficking are altered (Figure 5). The mechanism is clearly not transcriptional and probably not translational but rather post-translational. Although the full length E-cadherin cDNA was sequenced in MARY-X and MARY-X spheroids with no mutations found, alternate splicing or rearrangements (data not

shown), a translational component cannot be completely excluded to explain overexpression of E-cadherin. Certainly, altered translational regulation by ribosomal initiation factors or microRNAs could explain the overexpression but, they alone, would not explain the redistribution of E-cadherin observed 360º circumferentially around the cancer cell. This latter observation suggests the post-translational mechanism of altered trafficking. The present results showed that mRNAs encoding the endocytic trafficking regulators RAB7 and HRS are substantially decreased in the MARY-X spheroids compared to other E-cadherin-positive breast carcinoma cell lines, while EXOC5 mRNA is significantly increased compared to other E-cadherin-positive breast carcinoma cell lines. RAB7, a member of the Rab family, functions in the endocytic pathway of mammalian cells by regulating traffic from early to late endosomes. RAB7, specifically, is a monomeric GTPase, localized to multivesicular bodies and late endosomes, enhancing lysosome biogenesis (10). HRS, also referred to as hepatocyte growth factor-regulated tyrosine kinase substrate or HGS, is a ubiquitin-binding trafficking gatekeeper on sorting endosomes that controls the lysosomal degradation of ubiquitinated cargo such as endothelial growth factor receptors; its activity is regulated in turn by HRS tyrosine phosphorylation, ubiquitination, and degradation (11). Decreased RAB7 and HRS not only decreases lysosomal degradation but shuttles E-cadherin to the recycling endosomes (Figure 5). EXOC5 is a key component of the exocyst complex which also promotes endosomal recycling (Figure 5).

Lysosomal protein degradation may also involve ubiquitination. Ubiquitination is the conjugation of a 76 amino acid ubiquitin moiety to a target protein. This process has been reported to mark cellular proteins for proteasomal degradation (12, 13) and plasma membrane proteins for internalization, endocytic trafficking and lysosomal degradation (14-16). E-Cadherin is specifically thought to be ubiquitinated by the E3 ligase Hakai (17-19). Ubiquitinated E-cadherin is thought to be degraded in lysosomes after trafficking through RAB5- and RAB7-positive endosomal compartments (17). In these studies, the proteasome appeared to play an indirect role in E-cadherin degradation downstream of SRC activation (20). Interestingly, increased lysosomal targeting of E-cadherin has been postulated to represent a unique mechanism for the down-regulation of cell-cell adhesion during EMT (21). The present study is dealing with the opposite phenomenon, decreased lysosomal targeting for the up-regulation of cell-cell adhesion to foster the epithelial state.

Because it could be argued that both the increased EXOC5 and the decreased HRS and RAB7 were only correlative with E-cadherin overexpression, one of these molecules, RAB7, was arbitrarily chosen and targeted for knockdown. Similarly, HRS or overexpressed EXOC5 in MCF-7 could also have been chosen for knockdown in order to examine the effects on E-cadherin. RAB7 knockdown not only increased full-length E-cadherin but also induced the *de novo* appearance of the 95 KD E-cadherin fragment in MCF-7 cells, making the MCF-7 cells resemble the MARY-X spheroids more. This was additional proof that the molecules thought to regulate E-cadherin trafficking actually account for the unique E-cadherin post-translational processing and overexpression in the MARY-X spheroids. The 95 kDa fragment was not the only E-cadherin fragment observed in MARY-X and its derived spheroids. Understanding the nature and genesis of these other fragments may further elucidate the mechanisms of altered E-cadherin trafficking in IBC.

The present findings of decreased HRS and RAB7 and increased EXOC5 in the MARY-X spheroids were also observed in the lymphovascular tumoral emboli from human cases, suggesting that these observations have relevance *in vivo*.

The altered trafficking of E-cadherin in MARY-X spheroids and the lymphovascular emboli of both IBC as well as non-IBC cases, therefore, accounts for its overexpression and accumulation. E-cadherin accumulation and, subsequently, overexpression is responsible for both the formation of the MARY-X spheroids as well as the lymphovascular emboli and confers upon both structures a resistance to apoptosis and a survival advantage. It can be argued that, in the setting of the lymphovascular tumoral embolus, E-cadherin is functioning not as a suppressor gene but rather as an oncogene.

Acknowledgements

This study was supported by the Department of Defense Breast Cancer Research Program Grants BC990959, BC024258 and BC053405, the American Airlines–Susan Komen Promise Grant KG08128702 and the University of Nevada Vasco A. Salvadorini Endowment.

References

1 Berx G and Van Roy F: The E-cadherin/catenin complex: an important gatekeeper in breast cancer tumorigenesis and malignant progression. Breast Cancer Res *3*: 289-293, 2001.

2 Hajra KM, Chen DYS and Fearon ER: The slug zinc-finger protein represses E-cadherin in breast cancer. Cancer Res *62*: 1613-1618, 2002.

3 Lombaerts M, van Wezel T, Philippo K, Dierssen JWF, Zimmerman RME, Oosting J, van Eijk R, Eilers PH, van de Water B, Cornelisse CJ and Cleton-Jansen AM: E-cadherin transcriptional down-regulation by promoter methylation but not mutation is related to epithelial-to-mesenchymal transition in breast cancer cell lines. Br J Cancer *94*: 661-671, 2006.

4 Alpaugh ML, Tomlinson JS, Shao ZM and Barsky SH: A novel human xenograft model of inflammatory breast cancer. Cancer Res *59*: 5079-5084, 1999.

5 Tomlinson JS, Alpaugh ML and Barsky SH: An intact overexpressed E-cadherin/alpha, beta-catenin axis characterizes the lymphovascular emboli of inflammatory breast carcinoma. Cancer Res *61*: 5231-5241, 2001.

6 Alpaugh ML, Tomlinson JS, Kasraeian S and Barsky SH: Cooperative role of E-cadherin and sialyl-Lewis X/A-deficient MUC1 in the passive dissemination of tumor emboli in inflammatory breast carcinoma. Oncogene *21*: 3631-3643, 2002.
7 Alpaugh ML and Barsky SH: Reversible model of spheroid formation allows for high efficiency of gene delivery *ex vivo* and accurate gene assessment *in vivo*. Hum Gene Ther *13*: 1245-1258, 2002.
8 Alpaugh ML, Tomlinson JS, Ye Y and Barsky SH: Relationship of sialyl-Lewis x/a underexpression and E-cadherin overexpression in the lymphovascular embolus of inflammatory breast carcinoma. Am J Path *161*: 619-628, 2002.
9 Xiao Y, Ye Y, Yearsley K, Jones S and Barsky SH: The lymphovascular embolus of inflammatory breast cancer expresses a stem cell-like phenotype. Am J Path *173*: 561-574, 2008.
10 Bucci C, Thomsen P, Nicoziani P, McVarthy J and van Deurs B: Rab7: a key to lysosome biogenesis. Mol Cell Biol *11*: 467-480, 2000.
11 Stern KA, Visser Smit GD, Place TL, Winistorfer S, Piper RC and Lill NL: Epidermal growth factor receptor fate is controlled by Hrs tyrosine phosphorylation sites that regulate Hrs degradation. Mol Cell Biol *27*: 888-898, 2007.
12 Scheffner M, Huibregtse JM, Vierstra RD and Howley PM: The HPV-16 E6 and E6-AP complex functions as a ubiquitin-protein ligase in the ubiquitination of p53: Cell *75*: 495-505, 1993.
13 Ciechanover A: The ubiquitin-proteasome proteolytic pathway. Cell *79*: 13-21, 1994.
14 Hicke L. and Riezman H: Ubiquitination of a yeast plasma membrane receptor signals its ligand-stimulated endocytosis. Cell *84*: 277-287, 1996.
15 Roth A F and Davis NG: Ubiquitination of the yeast a-factor receptor. J Cell Biol *134*: 661-674, 1996.
16 Kolling R and Losko S: The linker region of the ABC-transporter Ste6 mediates ubiquitination and fast turnover of the protein. EMBO J *16*: 2251-2261, 1997.
17 Fujita Y, Krause G, Scheffner M, Zechner D, Leddy HE, Behrens J, Sommer T and Birchmeier W: Hakai, a c-Cbl-like protein, ubiquitinates and induces endocytosis of the E-cadherin complex. Nat Cell Biol *4*: 222-231, 2002.
18 Miyake S, Mullane-Robinson KP, Lill NL, Douillard P and Band H: Cbl-mediated negative regulation of platelet-derived growth factor receptor-dependent cell proliferation. A critical role for Cbl tyrosine kinase-binding domain. J Biol Chem *274*: 16619-16628, 1999.
19 Stern KA, Place TL and Lill NL: EGF and amphiregulin differentially regulate Cbl recruitment to endosomes and EGF receptor fate. Biochem J *410*: 585-594, 2008.
20 Miyake S, Lupher ML, Druker B and Band H: The tyrosine kinase regulator Cbl enhances the ubiquitination and degradation of the platelet-derived growth factor receptor alpha. Proc Natl Acad Sci USA *95*: 7927-7932, 1998.
21 Palacios F, Tushir JS, Fujita Y and D'Souza-Schorey C: Lysosomal targeting of E-cadherin: a unique mechanism for the down-regulation of cell-cell adhesion during epithelial to mesenchymal transitions. Mol Cell Biol *25*: 389-402, 2005.

Received July 29, 2010
Revised September 22, 2010
Accepted September 26, 2010